Title

Spurious Climate Impacts in Coupled Sea Ice Loss Simulations

Journal

Journal of Climate, 35(22)

ISSN

0894-8755

Authors

England, Mark R
Eisenman, Ian
Wagner, Till JW

Publication Date

2022-11-15

DOI

10.1175/jcli-d-21-0647.1

Peer reviewed

Spurious Climate Impacts in Coupled Sea Ice Loss Simulations

MARK R. ENGLAND,[a,b,c] IAN EISENMAN,[c] AND TILL J. W. WAGNER[b,d]

[a] *Department of Earth and Planetary Sciences, University of California, Santa Cruz, Santa Cruz, California*
[b] *Department of Physics and Physical Oceanography, University of North Carolina, Wilmington, North Carolina*
[c] *Scripps Institution of Oceanography, University of California, San Diego, San Diego, California*
[d] *Department of Atmospheric and Oceanic Sciences, University of Wisconsin–Madison, Madison, Wisconsin*

(Manuscript received 18 August 2021, in final form 21 July 2022)

ABSTRACT: Previous studies have used coupled climate model simulations with perturbed sea ice covers to assess the impact of future Arctic sea ice loss. The results of these studies suggest that Arctic sea ice loss will cause substantial climate impacts in the Arctic and beyond. The approaches used in these simulations can be broadly categorized into three methods: adding a ghost flux to the sea ice module, nudging, and modifying the surface albedo. Here we show that all three methods ultimately add heat to the Arctic in order to melt the sea ice, and that this artificial heating causes a spurious warming signal that is added to the warming that occurs due to sea ice loss alone. We illustrate this using an idealized climate model, which provides a preliminary rough estimate of the effect. In this model, the annual-mean warming due to sea ice loss alone can be directly calculated. We compare this with the warming that would be attributed to sea ice loss using each of the three methods in the idealized model. The results suggest that each method substantially overestimates the warming due to sea ice loss alone, overestimating the surface warming throughout the Northern Hemisphere by a factor of 1.5–2 in the idealized model. Hence, these results suggest that previous coupled climate modeling studies have overestimated the climate response to sea ice loss.

KEYWORDS: Sea ice; Climate change; Climate models; Idealized models

1. Introduction

The loss of Arctic sea ice is a prominent feature of observed climate change. Since 1979, the sea ice cover has diminished in every season and every basin across the Arctic Ocean, with the largest reduction occurring in September when approximately half the sea ice cover has been lost (Fetterer et al. 2017). The sea ice which remains is substantially thinner and younger, with the remaining thick multiyear ice being confined to a shrinking area in the central Arctic (Kwok 2018). Arctic sea ice is projected by comprehensive climate models to continue to decline over the coming decades (Collins et al. 2013; Senftleben et al. 2020; Notz et al. 2020). As a result, there has been substantial interest in understanding the potential impacts of Arctic sea ice loss on the climate system.

Coupled atmosphere–ocean climate models have been widely used to estimate the climate response to Arctic sea ice loss (Deser et al. 2015, 2016; Blackport and Kushner 2017; Screen et al. 2018; Sun et al. 2018; England et al. 2020a; Simon et al. 2021). Typically in such studies the Arctic sea ice cover is perturbed to match reduced ice conditions from a warmer climate, with the climate forcing otherwise unchanged, in order to separate the response to sea ice loss from the response to greenhouse gas increases. There is no agreed upon best practice for perturbing the sea ice cover in a coupled climate model configuration (Screen et al. 2018; Smith et al. 2019), and different studies have utilized a variety of methods. The most commonly used approaches to alter sea ice conditions in these studies can be categorized into the following three methods: ghost flux, nudging, and albedo modification. We here describe the main characteristics of each method (summarized in Table 1), noting that the details of the specific protocol implemented in each study differ.

Ghost flux: The ghost flux method refers to adding extra heat flux to the sea ice surface flux balance to replicate the desired sea ice state. This extra heat flux is only prescribed where sea ice is present. The flux is only seen directly by the sea ice component of the climate model, hence the name "ghost flux." Studies that use this method typically adopt the protocol outlined in Deser et al. (2015), in which the applied heat flux varies seasonally, with more flux per grid box required in the colder months. Implementing the ghost flux method requires carrying out a number of sensitivity experiments to determine the appropriate monthly heat flux values, before running the full simulation, because the heat flux field felt by the sea ice does not change during the full simulation. Previous studies have recognized that this method artificially adds heat into the high latitudes and thereby does not conserve energy, potentially causing a spurious response unrelated to sea ice loss (Deser et al. 2015; Screen et al. 2018).

Nudging: Direct nudging is used to constrain the area and the volume of Arctic sea ice to a target value. An aim of this approach is to accurately capture the full seasonal cycle of sea ice loss while minimizing the addition of artificial heat into the Arctic. For example, Smith et al. (2017) and Peings et al. (2021) nudged the sea ice state by simply removing sea ice to simulate the desired loss of sea ice concentration and

Supplemental information related to this paper is available at the Journals Online website: https://doi.org/10.1175/JCLI-D-21-0647.s1.

Corresponding author: Mark England, markengland@ucsc.edu

DOI: 10.1175/JCLI-D-21-0647.1

TABLE 1. Methods that have been widely used for constraining sea ice conditions in coupled climate model simulations and studies that implemented them.

Method	Description	Studies
Ghost flux	Additional heat flux is added to sea ice module alone	Deser et al. (2015, 2016); Tomas et al. (2016); Oudar et al. (2017); England et al. (2020a,b); Ringgaard et al. (2020)
Albedo modification	Albedo of sea ice is reduced to increase solar absorption	Scinocca et al. (2009); Deser et al. (2015); Blackport and Kushner (2016, 2017); Sévellec et al. (2017); Blackport et al. (2019); Simon et al. (2021)
Nudging	Sea ice is adjusted to constrain it to a desired state	McCusker et al. (2017); Smith et al. (2017); Sun et al. (2018, 2020); Peings et al. (2021)

thickness, with no direct perturbation to any model flux. This protocol is recommended by the Polar Amplification Model Intercomparison Project (PAMIP). Alternatively, McCusker et al. (2017), Sun et al. (2018), and Sun et al. (2020) instead constrained sea ice using "heat flux nudging." In this technique, at each time step the heat flux needed to melt the desired amount of sea ice is computed and then applied to the top (McCusker et al. 2017) or bottom (Sun et al. 2018, 2020) of the sea ice component. There are several differences between direct nudging and heat flux nudging in the coupled modeling framework, including that direct nudging does not conserve freshwater whereas heat flux nudging does. Similarly, Dai et al. (2019) specified the sea ice cover, which is equivalent to the direct nudging method in the limit of a fast relaxation time scale. In this configuration, the atmosphere and ocean components of the climate model saw the sea ice cover from the control run while CO_2 was ramped up.

Albedo modification: This refers to changing model parameters to reduce the sea ice albedo in order to cause sea ice loss through increased absorption of incoming solar radiation. All other climate forcing remains unchanged. For example, Blackport et al. (2019) reduced the albedo of cold, deep snow on top of sea ice such that the resulting summer sea ice cover was close to that obtained in a simulation with 2°C warming from greenhouse gases. One drawback of the albedo modification approach is that, although it can bring about substantial sea ice loss during the summer months, reducing the sea ice albedo has limited effects in polar winter and so the seasonal cycle of the sea ice loss can be heavily skewed (Blackport and Kushner 2016; Sun et al. 2020). On the other hand, a widely cited advantage of the albedo modification method is that it has been seen as conserving energy and thereby avoiding the main drawback of the ghost flux method (Blackport and Kushner 2016; Screen et al. 2018; Simon et al. 2021).

Note that in addition to these three broad methods, previous studies have occasionally adopted other approaches. For example, Petrie et al. (2015) and Semmler et al. (2016) performed simulations initialized in early summer with substantially thinner sea ice, which induces a loss of sea ice area throughout the rest of the year. Cvijanovic and Caldeira (2015) investigated a scenario of total sea ice loss in a slab ocean model configuration by artificially lowering the freezing point so that sea ice could not form. However, this approach cannot be directly applied to coupled simulations with an ocean equation of state. Simon et al. (2021) imposed sea ice loss by reducing the thermal conductivity of sea ice and the overlying snow. Some studies have attempted to infer the response to sea ice loss indirectly in simulations of greenhouse gas driven warming (Zappa et al. 2018; Ayres and Screen 2019; Screen and Blackport 2019), although causality is difficult to isolate using such statistical approaches. Last, other studies have prescribed sea ice loss in atmosphere-only simulations, but this approach does not conserve energy (see further discussion in section 4 below). We limit the scope of this study to investigating the three widely used methods for directly estimating the response to sea ice loss in coupled climate models described above.

Overall, these coupled sea ice loss simulations consistently have shown that Arctic sea ice loss causes a substantial warming and moistening of the northern high latitudes, especially close to the surface (Deser et al. 2015; Screen et al. 2018; Screen and Blackport 2019). In response to the reduced meridional temperature gradient associated with sea ice loss, the midlatitude tropospheric jet weakens on its poleward flank or shifts equatorward (Deser et al. 2015; Ronalds et al. 2018; Sun et al. 2018; Blackport et al. 2019). Notably, the coupled response to Arctic sea ice loss can extend to the tropics (Deser et al. 2015; Tomas et al. 2016; Wang et al. 2018; England et al. 2020a), with enhanced warming and precipitation in the equatorial regions, and it can even reach to the other pole (Deser et al. 2015; Liu and Fedorov 2019; England et al. 2020b).

It was previously suggested that the use of the different methods across different studies may produce a spread in the estimated response to sea ice loss (Cvijanovic et al. 2017; Smith et al. 2019). However, the three methods described above, when implemented in a range of coupled climate models, were found to produce results that were broadly consistent with one another, in terms of both the extratropical circulation and the thermodynamic response, after normalizing for the amount of sea ice loss (Screen et al. 2018). Similarly, in a study that directly tested how the choice of sea ice perturbation method impacts the simulated effects of sea ice loss, by performing sea ice loss simulations in a single climate model with a single ice loss target that used either albedo modification or nudging, the climate responses were found to be nearly identical (Sun et al. 2020). Thus, the different approaches are widely considered to be robustly isolating the climate response to sea ice loss. In fact, some recent studies have suggested, for reasons unrelated to the method used to perturb sea ice, that these simulations systematically underestimate the climate impacts of sea ice loss (e.g., Francis 2017; Mori et al. 2019; Cohen et al. 2020; Overland et al. 2021).

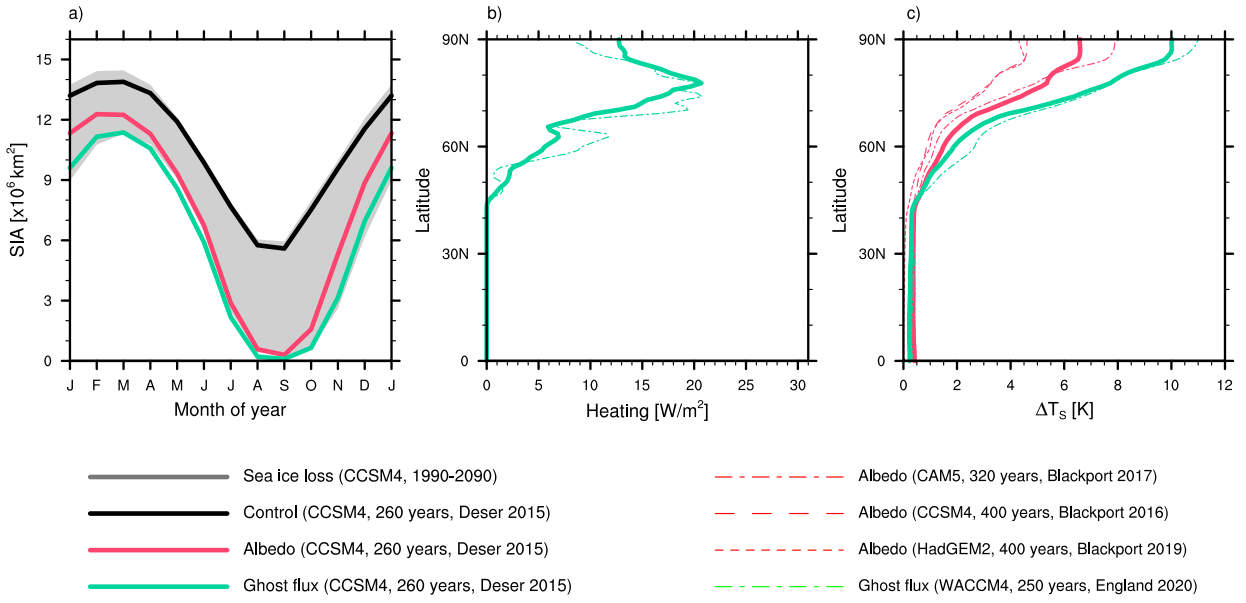

FIG. 1. Sea ice loss, heat input, and surface warming in coupled climate model simulations. (a) Seasonal cycle of Arctic sea ice area from the control (black), albedo modification (red), and ghost flux (green) CCSM4 simulations of Deser et al. (2015). The gray shading indicates the loss of sea ice area that the simulations are attempting to replicate. (b) The annual-mean artificial heating applied to achieve the targeted sea ice loss in the ghost flux simulations. It was not possible to estimate the artificial heating in the albedo modification simulations with the available simulation output. (c) The annual-mean surface warming attributed to Arctic sea ice loss in six sets of simulations. In (b) and (c), the fields are zonally averaged over ocean grid boxes. In all panels, albedo modification simulations are indicated in red and ghost flux simulations are indicated in green. The thicker solid lines show the Deser et al. (2015) simulations and the dashed lines show the other four sets of simulations, with the model, years of simulation averaged over, and the study indicated in the legend. The discrepancy between the top of the gray shading and the black line in (a) is due to difficulties in replicating a transient state in equilibrium-style simulations.

2. Artificial heating of the Arctic

In this study, we argue that there is a major limitation common to all three methods: in each approach a substantial artificial local heating is ultimately applied in the Arctic in order to melt the sea ice. This heating occurs through either direct changes to heat fluxes felt by the sea ice, the addition of absorbed solar radiation, or latent heat changes due to perturbing the sea ice volume. The effects of this heating are added to the direct effects of sea ice loss alone.

For the ghost flux and heat flux nudging methods, additional heat is explicitly added to the high latitudes. This issue has been identified in previous studies, although based on the similarity of the response to other methods, it has been argued that the additional heating has minimal effects (Sun et al. 2020). In the case of albedo modification, energy is added at the surface through changes in absorbed solar radiation, rather than directly through prescribed constant or computed fluxes. While this method technically conserves energy, it artificially increases the energy absorbed by the climate system. Last, the direct removal of ice thickness in the nudging procedure adds latent heat to the Arctic. This is because simply making ice disappear is essentially equivalent, in a climate model, to adding heat to the system and melting the ice. For example, adding sensible heat to the base of the sea ice which causes the ice to thin due to melting is energetically equivalent to achieving the same thinning by directly adjusting the ice thickness in the model, noting that the temperature at the ice–ocean interface is fixed at the melting point. Whatever form it takes, this added energy must ultimately be radiated to space. So it generates a warming of its own, separate from the climate response to sea ice loss.

We have collected coupled climate model output from six different sets of coupled sea ice loss simulations that were used in previous studies: four using the albedo modification method (Deser et al. 2015; Blackport and Kushner 2016, 2017; Blackport et al. 2019) and two using the ghost flux method (Deser et al. 2015; England et al. 2020a). Note that we were unable to acquire the necessary data from nudging simulations because the computed nudging values are not typically saved as output. Although each set of simulations uses slightly different protocols for choosing the control and future period, as well as the length of the simulation and exactly how the sea ice is constrained, for the case of the ghost flux simulations we can compute the amount of heating which is being added into the climate system. Figure 1a shows the seasonal cycle of Arctic sea ice area for the control run (black line) and the loss of sea ice area being replicated (the "target," gray shading), as well as the sea ice area after imposing the albedo modification method (red) and the ghost flux method (green) from the Deser et al. (2015) simulations. We highlight these two simulations of Deser et al. (2015) because they use the same control and future reference periods in the same climate model (CCSM4); the only difference is the ice perturbation

method. In this framework the control run is attempting to replicate the 1980–99 average Arctic sea ice conditions from CCSM4 historical simulations and the sea ice loss runs are attempting to replicate the 2080–99 average Arctic sea ice conditions from the model's RCP8.5 simulations. The Arctic sea ice loss simulated in the other studies we analyzed is shown in Fig. S1 in the online supplemental material.

In Fig. 1b we show the annual-mean zonal-mean heating added to constrain sea ice for the ghost flux method. Here, substantial artificial heating of over 10 W m^{-2} is applied to the Arctic, peaking at approximately 20W m^{-2} close to the pole. Artificial heating is also (indirectly) added for the albedo modification method through altering the absorbed shortwave flux. However, we were not able to estimate from the available simulation output how much of the total change in absorbed shortwave flux is attributable to the true role of sea ice loss, including via the sea ice–albedo feedback, and how much is attributable to artificial heating. Figure 1c shows the latitudinal structure of the annual-mean zonal-mean surface warming that is attributed to Arctic sea ice loss in these studies. The surface warming of is largest in the very high latitudes, reaching 10 K in the ghost flux simulations and 4–8 K in the albedo modification simulations. The larger surface warming in the ghost flux simulations than the albedo modification simulations is expected because the imposed annual-mean sea ice loss is smaller in the albedo modification simulations (Fig. 1a). This warming was previously attributed entirely to sea ice loss. Here we argue that some of this warming must have resulted instead from the artificial heating that was added to melt the ice in these simulations. In what follows, we discuss how much of this substantial surface warming can be attributed to sea ice loss alone by drawing on an idealized climate model.

3. Idealized climate model

We use an idealized climate model to illustrate the effects of the artificial heating that is imposed in the comprehensive climate model simulations and to generate a rough approximation of how much extra warming it causes. By implementing the three different methods in the idealized climate model, we can more concretely investigate the effects of the artificial heating that they add. It is important to emphasize that we are not using this idealized model as an attempt to quantify the role of sea ice loss more accurately than in a comprehensive climate model, but rather to explore a proposed deficiency in a class of climate model methods. Crucially, in this idealized climate model the direct effect of sea ice loss can be directly calculated, as discussed below.

a. Model formulation

We utilize the idealized model developed by Wagner and Eisenman (2015a, hereafter WE15). This model simulates the seasonally varying evolution of surface temperature and sea ice thickness as a function of latitude on a zonally uniform aquaplanet. The model describes an ice-free ocean mixed layer when the surface is above the freezing point, and it represents a layer of sea ice with varying thickness when the surface is at or below the freezing point. Variations of this model have been previously used to study a range of different phenomena including the stability of the sea ice cover in a warming climate (WE15; Wagner and Eisenman 2015b), Arctic amplification (Merlis and Henry 2018; Beer et al. 2020; Feldl and Merlis 2021), the seasonal cycle of Antarctic sea ice (Roach et al. 2022), and the effects on the sea ice cover of atmospheric and oceanic heat transport (Aylmer et al. 2020) and sea ice drift (Wagner et al. 2021).

The model simulates the evolution of the enthalpy $E(t, \theta)$ of the surface and overlying atmospheric column as a function of time t and latitude θ, governed by

$$\frac{\partial E}{\partial t} = (1 - \alpha)S - [A + B(T_s - T_f)] + D\nabla^2 T_s + F + F_b, \tag{1}$$

where $\alpha(E, \theta)$ is the surface albedo, $S(t, \theta)$ is incoming solar radiation at the top of atmosphere, $T_s(t, \theta)$ is the surface temperature, T_f is the freezing point, $A + B(T_s - T_f)$ is a linear representation of outgoing longwave radiation (cf. Koll and Cronin 2018) with constants A and B, $D\nabla^2 T_s$ is a diffusive approximation of meridional heat transport with constant diffusivity D, F is a spatially uniform and seasonally constant climate forcing that can be interpreted as representing the radiative forcing from CO_2, and F_b is the upward heat flux from the deep ocean to the ocean surface mixed layer. The state of the system is determined by the enthalpy of the surface, assuming that the atmospheric column has negligible heat capacity. When E is positive, open ocean is present; and when E is negative, the ocean is covered with sea ice of thickness $h = -E/L_f$, where L_f is the latent heat of fusion. The surface temperature is given by

$$T_s = \begin{cases} T_f + \dfrac{E}{c_w}, & E > 0 \quad \text{(open water)} \\ T_f, & E < 0,\ T_0 > T_f \ \text{(melting ice)} \\ T_0, & E < 0,\ T_0 < T_f \ \text{(freezing ice)} \end{cases}, \tag{2}$$

where T_0 is the ice surface temperature required to balance the surface energy flux, and c_w is the heat capacity of the ocean mixed layer. The surface albedo is given by

$$\alpha = \begin{cases} \alpha_0 + \alpha_2 \sin^2\theta, & E > 0 \ \text{(open water)} \\ \alpha_i, & E < 0 \ \text{(ice)} \end{cases}, \tag{3}$$

with empirical parameters $\alpha_0 = 0.3$, $\alpha_2 = 0.1$, and $\alpha_i = 0.6$. Each grid cell of the model approximately represents the energetic state of the entire atmosphere–ocean–sea ice column. The model accounts for energy entering, leaving, and stored in the column, but it does not resolve processes which transfer heat within the column (such as surface turbulent heat fluxes).

In this model, sea ice influences climate in two distinct ways: (i) insulation effects, which depend on whether sea ice is present and its thickness h, and (ii) surface albedo effects, which only depend on whether sea ice is present [Eq. (3)]. The heat flux across the equator is approximated to be zero,

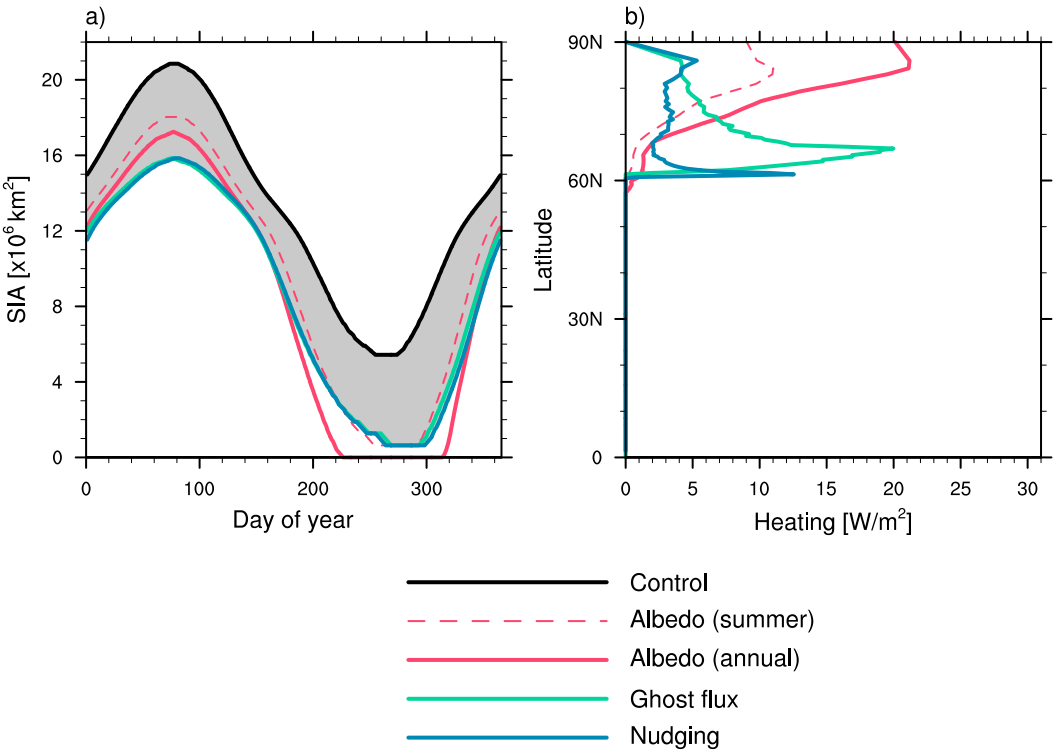

FIG. 2. (a) Seasonal cycle of sea ice area in the WE15 simulations. The black line indicates the CONTROL simulations, and the gray shading indicates the change of sea ice area from CONTROL to FUTURE. The colored lines show the sea ice area after applying the different methods for imposing sea ice loss, with the target being the sea ice area from the FUTURE simulation. Here the sea ice area is computed as the sum of the real-world ocean areas in all latitude bands associated with model grid boxes that are simulated to have sea ice present, thereby incorporating the distribution of landmasses, which is not explicitly accounted for in the WE15 model formulation. (b) The latitudinal profile of the annual-mean surface heating artificially applied in the sea ice loss simulations.

which allows the domain to be restricted to a single hemisphere. See WE15 for further details regarding this model.

We run the model using the default parameter values outlined in Table 1 of WE15, which simulate an observationally consistent modern climate of the Northern Hemisphere. Each simulation is run for 200 years, reaching an approximate equilibrium, and the output from the final year is analyzed. We perform two baseline simulations. The first is a control run, hereafter referred to as CONTROL, which has a climate forcing of $F = 0$ and simulates present-day Arctic sea ice conditions (Fig. 2a, black line). Note that the idealized model approximately replicates the observed summer sea ice minimum but simulates a somewhat larger wintertime sea ice area than the observed present-day Arctic. The second simulation is of a warmer climate, hereafter referred to as FUTURE, using a climate forcing $F = 3.1$ W m^{-2} which approximates end-of-century Arctic sea ice loss typical under high emissions scenarios as simulated by comprehensive climate models. Here in order to facilitate a more direct comparison of sea ice area between the aquaplanet setup in the idealized model and the comprehensive climate model simulations which contain realistic continental landmasses, we have computed the sea ice area from the idealized model simulations after weighting each meridional grid box by the fraction of the associated latitude band that has ocean in the real climate system (i.e., adopting the perspective of Eisenman (2010) to convert the simulated aquaplanet sea ice area into an implied sea ice area in the presence of continents).

b. *Annual-mean response to sea ice loss*

A key benefit of this idealized model for the present purposes is that, in the annual mean, the role of sea ice loss can be directly diagnosed. This is because taking the annual mean of Eq. (1), which we denote with an overbar, at equilibrium (such that $\partial\overline{E}/\partial t = 0$) we are left with

$$A + B(\overline{T_s} - T_f) - D\nabla^2\overline{T_s} - F - F_b = \overline{(1-\alpha)S}, \qquad (4)$$

and the annual-mean surface temperature can be determined by solving Eq. (4) for $\overline{T_s}$. We decompose the surface temperature response $\Delta\overline{T_s}$ to a change in climate forcing ΔF into the Northern Hemisphere mean warming $\Delta\langle\overline{T_s}\rangle$ and the deviation from this $\Delta\overline{T}_s'$, such that $\Delta\overline{T_s} = \Delta\langle\overline{T_s}\rangle + \Delta\overline{T}_s'$. Here, angle brackets indicate the hemispheric average, and the prime indicates deviations from it. In this fashion, the annual-mean

TABLE 2. Description of simulations performed using the WE15 idealized climate model.

Simulation	Climate forcing F (W m^{-2})	Modification
CONTROL	0.0	None
FUTURE	3.1	None
SPECIFIED_ALBEDO	0.0	Surface albedo specified from FUTURE
GHOST_FLUX	0.0	$35 + 30\sin[2\pi(t + 5)]$ W m^{-2}, where t is time in years, applied to ice-covered grid boxes that are ice-free in FUTURE
ALBEDO$_{summer}$	0.0	Albedo of sea ice reduced from $\alpha_i = 0.6$ to 0.55
ALBEDO$_{annual}$	0.0	Albedo of sea ice reduced from $\alpha_i = 0.6$ to 0.52
NUDGING	0.0	Enthalpy reduced to zero in ice-covered grid boxes that are ice-free in FUTURE with a time scale of 7 days

hemispheric-mean surface temperature response can be calculated from the hemispheric mean of Eq. (4) as

$$\Delta\langle\overline{T_s}\rangle = \frac{\Delta F - \Delta\langle\overline{\alpha S}\rangle}{B}, \tag{5}$$

where $\Delta\langle\overline{\alpha S}\rangle$ is the hemispheric-mean change in absorbed solar radiation due to surface albedo changes. Hence, from the hemispheric-mean perspective, the annual-mean surface temperature response is determined solely by the climate forcing and the warming from the surface albedo feedback.

It is less straightforward to compute $\Delta\overline{T}_s'$, the latitudinal structure of the warming response, but it can be written in an implicit form:

$$B\Delta\overline{T}_s' - D\nabla^2(\Delta\overline{T}_s') = -\Delta\overline{\alpha S}'. \tag{6}$$

Thus, the annual-mean latitudinal structure of the surface temperature response is solely attributable to sea ice loss through the change in surface albedo α. The detailed derivation of Eqs. (5) and (6) is included in Text S1 of the supplemental material.

Crucially, taking Eqs. (5) and (6) together, the only effect sea ice loss has on the annual-mean surface temperature response $\Delta\overline{T_s}$ is through changes in the surface albedo α. The annual-mean surface temperature does not depend on sea ice thermodynamic effects, which are embodied in the relationship between T_s and E [Eq. (2)]. This occurs in the idealized model because of the approximation that outgoing longwave radiation is linear in T_s with a spatially constant coefficient B, implying a spatially uniform value of all climate feedback parameters other than surface albedo, which would not be the case in a comprehensive climate model. Changes in sea ice thickness influence the seasonal cycle of surface temperature in this model ($T_s - \overline{T_s}$), but not the annual-mean value, which responds solely to the change in surface albedo. Knowing the actual effects of sea ice loss in this model allows us to evaluate the performance of the three widely used sea ice perturbation methods.

Hence, to simulate the actual impact of sea ice loss in the idealized model, we run a third simulation, identical to the CONTROL run except with the surface albedo specified from the FUTURE run. This simulation will be hereafter referred to as SPECIFIED_ALBEDO. From an annual-mean perspective, the difference between SPECIFIED_ALBEDO and CONTROL is exactly equal to the effect of sea ice loss alone. From Eq. (5), the SPECIFIED_ALBEDO simulation imposes $\Delta F = 0$ but specifies the change in surface albedo associated with $\Delta F = 3.1$ W m^{-2}. In the annual-mean, the only nonlinearity in this model arises from the ice albedo feedback. Hence, the difference in annual-mean temperature between the FUTURE simulation and the SPECIFIED_ALBEDO simulation is the latitudinally uniform warming that would occur in the absence of sea ice loss, which is readily computed from Eqs. (5) as $\Delta T_s = \Delta F/B = (3.1\text{ W m}^{-2})/(2.1\text{ W m}^{-2}\text{ K}^{-1}) = 1.5$ K. Thus, the role of sea ice loss in the annual-mean surface temperature response in this model is both relatively straightforward to diagnose and intuitive to understand.

It is important to note that specifying the albedo in this way is not the same as the albedo modification method, in which sea ice parameters are altered to achieve the desired amount of sea ice loss. In the albedo modification method, there is heating from the change in albedo where sea ice is lost (which is the actual impact of the ice loss) and additionally from the imposed reduction in albedo in locations where sea ice remains (which is the artificial heating required in addition to sustain the targeted reduction in sea ice cover), whereas the SPECIFIED_ALBEDO simulation only has heating from the former.

c. *Implementing sea ice loss simulation methods in the idealized model*

The idealized model offers a framework to illustrate the effects of the three standard sea ice perturbation methods, outlined in section 1, and their effects on the climate system. These methods are applied such that the sea ice conditions from the FUTURE run (bottom edge of gray shading in Fig. 2a) are matched while using climate forcing from the CONTROL run. The differences between these simulations and the CONTROL run will represent the climate impact of sea ice loss as estimated using the standard approaches. In the implementation of these methods in the idealized model, we stay as close as possible to the original protocol in the comprehensive climate modeling framework. Note that although we constrain only the sea ice area, the sea ice volume is also fairly well replicated (not shown). The idealized model simulations used in this study are summarized in Table 2.

Ghost flux: To replicate the ghost flux method, an additional flux is added to areas currently covered by sea ice which transition to ocean covered in the FUTURE simulation. This is designed to mimic the approach of Deser et al. (2015) and England et al. (2020a) in which the additional flux is applied only to the surface of the sea ice module. As in those studies, the ghost flux is seasonally varying. Here, the applied flux has an annual average value of 35 W m^{-2} and varies sinusoidally between a maximum of 65 W m^{-2} in the winter and a minimum of 5 W m^{-2} in the summer. To achieve a realistic retreat of the sea ice edge, ghost flux is also applied in areas covered by thin sea ice in the FUTURE simulation which we define as $E > -3$ W m^{-2} yr (an ice thickness of 30 cm). This adjustment is analogous to the representation in the comprehensive models where a grid box that transitions to thin ice experiences some reduction in the sea ice concentration and hence has a ghost flux applied to it. This simulation will be referred to hereafter as GHOST_FLUX. By design, the GHOST_FLUX simulation is able to approximately simulate the seasonal cycle of the reduction in sea ice area (Fig. 2a, green line).

Nudging: As discussed in section 1, there are two types of nudging: direct nudging and heat flux nudging. To replicate the direct nudging method, we constrain the sea ice area in the CONTROL run to that of the FUTURE run by removing sea ice from grid boxes where sea ice is currently present but there is open ocean in the FUTURE run, using a Newtonian relaxation time scale of 7 days. To replicate heat flux nudging in this model, we instead nudge the enthalpy to be just above zero in grid boxes where sea ice is currently present but there are ice-free conditions in the FUTURE run, again using a Newtonian relaxation time of 7 days. Although these two techniques are implemented differently in comprehensive climate models, in the idealized model they end up being identical because it is the same to heat the surface and melt all the ice as it is to directly remove all the ice. We will refer to these simulations in our framework as NUDGING. By design, the NUDGING simulations capture the full seasonal cycle of the reduction in sea ice area (Fig. 2a, blue line).

Albedo modification: Previous studies have shown that the albedo modification method is unable to closely approximate the seasonal cycle of projected Arctic sea ice loss (Deser et al. 2015). Summer sea ice loss is readily achieved through the increase in absorbed solar radiation, but there is limited sea ice reduction in the dark winter months. Therefore, a choice has to be made between matching the summer sea ice loss or matching the annual-mean sea ice loss, with previous studies opting to pursue the former strategy (Deser et al. 2015; Blackport et al. 2019). To replicate the albedo modification method, we reduce the albedo of sea ice from $\alpha_i = 0.6$ to 0.55. This simulation, hereafter referred to as $\text{ALBEDO}_{\text{summer}}$, matches the summer sea ice minimum from FUTURE but only induces 53% of the targeted sea ice loss in winter (Fig. 2a, dashed red line). Using this method, the annual-mean sea ice area loss is underestimated by 25%. We implement a second albedo modification method, hereafter referred to as $\text{ALBEDO}_{\text{annual}}$, which targets the annual-mean sea ice loss. In this simulation we reduce the albedo of sea ice from $\alpha_i = 0.6$ to $\alpha_i = 0.52$. This results in 70% of the targeted winter sea ice loss but excessive ice loss in the summer, which balances out to match the targeted annual-mean sea ice area loss of 4.7×10^6 km^2 (Fig. 2a, solid red line).

We next consider the artificial heating applied in the different methods as implemented in the idealized model. As in the computation of ice area in the idealized model, we weight each meridional grid box by the fraction of the associated latitude band that has ocean in the real world. The artificial annual-mean heating from the ghost flux and nudging methods are directly calculated from the heat flux applied at each time step to constrain the sea ice. The imposed artificial annual-mean heating from the albedo modification method is calculated from the additional solar radiation absorbed at the surface due to the imposed changes in surface albedo. We find that the heating profiles in the idealized model simulations are broadly consistent with the comprehensive model results (cf. Figs. 1b and 2b). For example, one similarity is that the peak of the applied heating in the ghost flux simulations occurs not directly at the pole but farther southward, coinciding with the region of most substantial sea ice area loss. However, more heating is applied at lower latitudes in the idealized model compared to the comprehensive climate model simulations. There are some noticeable differences between the heating profiles of the different methods within the idealized model. For example, the nudging method adds most of the heat near the CONTROL winter sea ice edge to constrain the sea ice area. By contrast, the albedo modification method adds heat predominantly at the higher latitudes where the remaining sea ice cover artificially absorbs a substantial amount of incoming solar radiation due to the modified albedo parameters. Also note that the disparity between the heating added by the ghost flux method and by the nudging method appears to be due to the difference in heating added to grid cells containing a thin layer of sea ice: a large fixed heating in the case of ghost flux versus a smaller computed heating in the case of nudging. Despite these differences, it is clear that all of the methods are adding substantial artificial heating to the Arctic climate in the idealized model, similar to the comprehensive climate models.

4. Results and discussion

Here we examine the surface temperature response in the idealized model simulations. We begin by considering the latitudinal profile of the total surface warming in response to the climate forcing increasing to $F = 3.1$ W m^{-2}, i.e., the difference between the FUTURE and CONTROL simulations (Fig. 3, black line). The temperature response is characterized by an annual-mean Northern Hemisphere warming of 2.2 K with an enhanced polar warming. Note that the polar amplification of this warming in the idealized model occurs due to surface albedo changes alone, as shown in Eq. (6) above. The warming caused by sea ice loss alone in this model is given by the difference between the SPECIFIED_ALBEDO and CONTROL simulations (Fig. 3, gray line). Note that the difference between the gray and black lines in Fig. 3, which represents the response to radiative forcing with no albedo change, takes the spatially uniform value $\Delta\overline{T_s} = 1.5$ (see

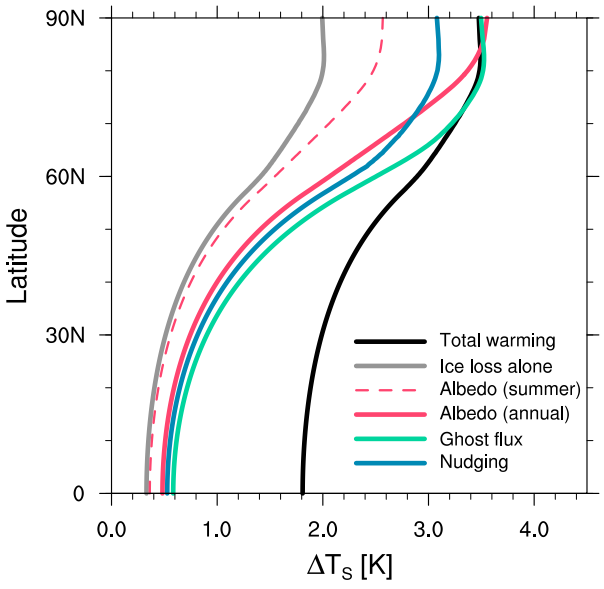

FIG. 3. Latitudinal profile of the annual-mean surface temperature response to Arctic sea ice loss in WE15. The black line is the total warming under 3.1 W m^{-2} of radiative forcing (FUTURE − CONTROL). The gray line is the warming attributable to sea ice loss alone (SPECIFIED_ALBEDO − CONTROL). The colored lines show the surface temperature response to sea ice loss as estimated using the different methods. For example, the blue line shows the surface temperature response as estimated using the nudging method (NUDGING − CONTROL). Note that these methods are all attempting to estimate the gray line.

explanation in section 3b above). It should be noted that the response to sea ice loss alone in this model is not expected to be a precise estimate of the response in comprehensive models or in nature; evidence from previous comprehensive modeling studies (e.g., Graversen and Wang 2009; Langen et al. 2012; Rose et al. 2014; Russotto and Biasutti 2020) suggests that the latitudinal structure of the warming absent sea ice loss should be polar amplified in comprehensive climate models, although a recent study found conflicting results (Shaw and Smith 2022). Next, we compare the estimates from the different methods to the true response to sea ice loss in this model.

As expected due to the artificial heating discussed in section 2, each method overestimates the annual-mean surface temperature response to Arctic sea ice loss (cf. the colored lines with the gray line in Fig. 3). Considering only the methods that target the annual-mean level of sea ice loss, we find that the surface warming is overestimated by a factor that varies spatially over the range 1.5–2 in the idealized model. Even the $ALBEDO_{summer}$ simulation, which only simulates 75% of the targeted annual-mean sea ice loss, overestimates the surface warming at all latitudes, albeit by a smaller amount than the methods which give the full annual-mean loss. We note that if a constant flux is implemented in the GHOST_FLUX simulations instead of the time-varying flux, it leads to an even larger overestimation (not shown).

In high latitudes, the solid colored lines in Fig. 3 approximately line up with the solid black line, indicating that the three methods give approximately the same level of warming in the Arctic as in the FUTURE simulation. This is because they are simulating the warming that occurs in response to (i) the heating that is required to melt the ice plus (ii) the heating from the surface albedo change due to the sea ice loss, which is similar to the Arctic heating in the FUTURE simulation. The Arctic warming that occurs due to the heating from sea ice loss alone is considerably smaller (gray line in Fig. 3). Note that in the SPECIFIED_ALBEDO simulation (gray line in Fig. 3) and the three methods (solid colored lines in Fig. 3), heating is applied only in the Arctic, which causes a warming in the Arctic that is transmitted to lower latitudes by changes in the meridional heat transport (simulated as linear diffusion in the idealized model). Hence, the meridional structure of the warming is similar in all four runs (gray line and solid colored lines in Fig. 3), although it is scaled by a factor of 1.5–2 in the runs that artificially heat the Arctic (colored lines in Fig. 3).

Although the present study focuses on widely used coupled climate model methods, many previous studies have also investigated the impacts of sea ice loss using atmosphere-only simulations. In these simulations, the sea ice cover is prescribed as a boundary condition, and the artificial heating concerns raised here do not apply. Intriguingly, Deser et al. (2015) found that the high-latitude warming attributed to sea ice loss in atmosphere-only simulations was within 10% of coupled climate model results that used the ghost flux method. However, energy is explicitly not conserved in these atmosphere-only simulations, and this and related issues motivated investigations of sea ice impacts to largely transition to coupled climate model simulations. It is a topic of continuing research whether atmosphere-only simulations can be used to help address the spurious climate impacts in coupled climate model simulations that are identified in the present work.

Consistent with previous studies that used comprehensive climate models (Screen et al. 2018; Sun et al. 2020), we find that there is relatively good agreement among the different methods in their estimates of the surface temperature response to sea ice loss. We note that we find similar overall results when the effects of sea ice loss are estimated using a simulation of FUTURE climate with sea ice conditions fixed to CONTROL conditions (see Text S2 for further details). We emphasize that the nudging method does not avoid the shared limitation because the additional latent heat will need to be balanced, after any transient response related to the sensible and latent heat content of the system, by an anomaly in outgoing longwave radiation (see Fig. S2 for a demonstration of this).

The approach we used to isolate the true response to sea ice loss in the idealized model cannot be directly replicated in a more complex model in which the surface energy balance is not linearly dependent on the surface temperature (since otherwise sea ice thickness changes can influence the annual-mean response) and effects of brine rejection are included. Furthermore, note that the magnitude of Arctic warming is relatively small in the idealized model compared

to comprehensive climate model simulations. The main reason for this is that both the climate sensitivity and the Arctic amplification factor are relatively low in this model. First, the simulated hemispheric-mean warming of 2.2 K under a radiative forcing of 3.1 W m^{-2} (Fig. 3, black line), when combined with the approximate radiative forcing due to doubling CO_2 of 3.7 W m^{-2} (e.g., Ramaswamy et al. 2001), implies an equilibrium climate sensitivity in the idealized model of 2.6 K. This lies near the lower end of the likely range of 2.6–3.9 K found in the recent work of Sherwood et al. (2020). Second, in the idealized model, the ratio of Arctic warming (3.4 K) to tropical warming (1.8 K) gives an Arctic amplification factor of 1.9, which is on the low end of the range simulated by the current generation of comprehensive climate models (approximately 1.5–4.0) (Cai et al. 2021). This is not surprising, since many of the processes which are thought to positively contribute to Arctic amplification, such as the lapse rate and cloud feedbacks and latent heat transport changes, are not included in this model.

It should be emphasized by caveat that this model lacks representations of many important processes in the climate system, including changes in clouds, atmospheric moisture, atmospheric circulation, snow cover on sea ice, sea ice motion, sea ice brine rejection, ocean circulation, spatial and temporal changes in the strength of climate feedbacks, and many other factors. Thus the factor of 1.5–2 in Fig. 3 should be taken as a back-of-the-envelope estimate rather than an accurate quantitative assessment. Nonetheless, if these methods do not work in an idealized model like this one, it seems unlikely that they would work any better in a comprehensive climate model.

5. Conclusions

The results of this study suggest that the standard methods used to isolate the climate response to sea ice loss in previous coupled climate modeling studies overestimate the impact of sea ice loss. This is because these methods all artificially heat the high latitudes in order to melt the ice, which causes a warming in addition to the impact of sea ice loss alone. We show that similar artificial heating occurs whether the heating is applied directly as an imposed flux, such as in the ghost flux methods, or indirectly, such as in the albedo modification method. We show that this also occurs similarly when no heat is explicitly added but instead ice is simply removed using the direct nudging method, because this is equivalent to adding latent heat. We illustrate these arguments using an idealized climate model, in which the actual impact of sea ice loss can be directly calculated and compared with estimates generated by using the standard method. In the idealized model framework these methods all overestimate the annual-mean impact of sea ice loss on surface warming by a factor of 1.5–2. Although this idealized model result should be taken as a back-of-the-envelope estimate rather than an accurate quantitative assessment, it suggests that the wide range of impacts of sea ice loss on the climate system that have been previously identified in coupled climate modeling studies, such as impacts on the midlatitude tropospheric jet and on the position and strength of the tropical rain belts, may be similarly overestimated and warrant further study. Understanding the precise magnitude of the overestimation in a comprehensive climate modeling framework is a topic of continuing research.

These results imply that careful interpretation is required with regards to previously published sea ice loss simulations with coupled climate models in light of the imposed artificial heating identified here. They appear to overestimate the impact of sea ice loss, but they have direct implications regarding the climate response to an imposed heating in the Arctic, with relevance to how Arctic climate change is connected to the rest of the globe.

These idealized climate model results do not robustly determine which of the previously used methods performs best or exactly how much each overestimates the impact of sea ice loss. And to this end, we do not propose an alternative method to accurately isolate all aspects of how sea ice loss impacts the climate system without ultimately adding heat in order to remove the ice. Nonetheless, the present study does illuminate one potential way of tackling this research question, which would require a slight change in perspective. Instead of focusing on the comprehensive impact of sea ice loss using a single approach, coupled comprehensive climate model simulations could be used to investigate the role of specific processes related to sea ice loss. For example, the influence of sea ice loss on the climate system due to changes in albedo could be investigated using comprehensive climate models with the surface albedo specified (e.g., Hall 2004). Alternatively, the climate impacts of the freshwater flux associated with sea ice loss can be readily investigated with a type of freshwater hosing experiment (e.g., Sime et al. 2019). Both examples rely on techniques that have been utilized previously and avoid the addition of artificial heating. A set of simulations from a single climate model which explore the roles of these various processes in a coordinated manner would help to improve our understanding on the role of sea ice loss while avoiding the spurious climate impacts identified in this study.

Acknowledgments. We thank Russell Blackport and three anonymous reviewers for help improving this manuscript. Without implying their endorsement, we also thank Clara Deser and Lantao Sun for illuminating discussions, which helped to frame this work. We are grateful to Lantao Sun, Stephanie Hay, and Russell Blackport for making model simulation output available for this study.

Data availability statement. The code for running the idealized model and reproducing the analysis and figures in this study is available at https://eisenman-group.github.io/.

REFERENCES

Aylmer, J., D. Ferreira, and D. Feltham, 2020: Impacts of oceanic and atmospheric heat transports on sea-ice extent. *J. Climate*, **33**, 7197–7215, https://doi.org/10.1175/JCLI-D-19-0761.1.

Ayres, H., and J. Screen, 2019: Multimodel analysis of the atmospheric response to Antarctic sea ice loss at quadrupled CO_2.

Geophys. Res. Lett., **46**, 9861–9869, https://doi.org/10.1029/2019GL083653.

Beer, E., I. Eisenman, and T. Wagner, 2020: Polar amplification due to enhanced heat flux across the halocline. *Geophys. Res. Lett.*, **47**, e2019GL086706, https://doi.org/10.1029/2019GL086706.

Blackport, R., and P. Kushner, 2016: The transient and equilibrium climate response to rapid summertime sea ice loss in CCSM4. *J. Climate*, **29**, 401–417, https://doi.org/10.1175/JCLI-D-15-0284.1.

——, and ——, 2017: Isolating the atmospheric circulation response to Arctic sea ice loss in the coupled climate system. *J. Climate*, **30**, 2163–2185, https://doi.org/10.1175/JCLI-D-16-0257.1.

——, J. Screen, K. van der Wiel, and R. Bintanja, 2019: Minimal influence of reduced Arctic sea ice on coincident cold winters in mid-latitudes. *Nat. Climate Change*, **9**, 697–704, https://doi.org/10.1038/s41558-019-0551-4.

Cai, S., P. Hsu, and F. Liu, 2021: Changes in polar amplification in response to increasing warming in CMIP6. *Atmos. Oceanic Sci. Lett.*, **14**, 100043, https://doi.org/10.1016/j.aosl.2021.100043.

Cohen, J., and Coauthors, 2020: Divergent consensuses on Arctic amplification influence on midlatitude severe winter weather. *Nat. Climate Change*, **10**, 20–29, https://doi.org/10.1038/s41558-019-0662-y.

Collins, M., and Coauthors, 2013: Long-term climate change: Projections, commitments and irreversibility. *Climate Change 2013: The Physical Science Basis*, T. F. Stocker et al., Eds., Cambridge University Press, 1029–1136.

Cvijanovic, I., and K. Caldeira, 2015: Atmospheric impacts of sea ice decline in CO_2 induced global warming. *Climate Dyn.*, **44**, 1173–1186, https://doi.org/10.1007/s00382-015-2489-1.

——, B. Santer, C. Bonfils, D. Lucas, J. Chiang, and S. Zimmerman, 2017: Future loss of Arctic sea ice cover could drive a substantial decrease in California's rainfall. *Nat. Commun.*, **8**, 1947, https://doi.org/10.1038/s41467-017-01907-4.

Dai, A., D. Luo, M. Song, and J. Liu, 2019: Arctic amplification is caused by sea-ice loss under increasing CO_2. *Nat. Commun.*, **10**, 121, https://doi.org/10.1038/s41467-018-07954-9.

Deser, C., R. Tomas, and L. Sun, 2015: The role of ocean–atmosphere coupling in the zonal-mean atmospheric response to Arctic sea ice loss. *J. Climate*, **28**, 2168–2186, https://doi.org/10.1175/JCLI-D-14-00325.1.

——, L. Sun, R. Tomas, and J. Screen, 2016: Does ocean coupling matter for the northern extratropical response to projected Arctic sea ice loss? *Geophys. Res. Lett.*, **43**, 2149–2157, https://doi.org/10.1002/2016GL067792.

Eisenman, I., 2010: Geographic muting of changes in Arctic sea ice cover. *Geophys. Res. Lett.*, **37**, L16501, https://doi.org/10.1029/2010GL043741.

England, M., L. Polvani, L. Sun, and C. Deser, 2020a: Tropical climate responses to projected Arctic and Antarctic sea ice loss. *Nat. Geosci.*, **13**, 275–281, https://doi.org/10.1038/s41561-020-0546-9.

——, L. M. Polvani, and L. Sun, 2020b: Robust Arctic warming caused by projected Antarctic sea ice loss. *Environ. Res. Lett.*, **15**, 104005, https://doi.org/10.1088/1748-9326/abaada.

Feldl, N., and T. Merlis, 2021: Polar amplification in idealized climates: The role of ice, moisture, and seasons. *Geophys. Res. Lett.*, **48**, e2021GL094130, https://doi.org/10.1029/2021GL094130.

Fetterer, F., W. Meier, M. Savoie, and A. Windnagel, 2017: Sea ice index, version 3. NSIDC, accessed 22 March 2022, https://nsidc.org/data/seaice_index.

Francis, J., 2017: Why are Arctic linkages to extreme weather still up in the air? *Bull. Amer. Meteor. Soc.*, **98**, 2551–2557, https://doi.org/10.1175/BAMS-D-17-0006.1.

Graversen, R., and M. Wang, 2009: Polar amplification in a coupled climate model with locked albedo. *Climate Dyn.*, **33**, 629–643, https://doi.org/10.1007/s00382-009-0535-6.

Hall, A., 2004: The role of surface albedo feedback in climate. *J. Climate*, **17**, 1550–1568, https://doi.org/10.1175/1520-0442(2004)017<1550:TROSAF>2.0.CO;2.

Koll, D., and T. Cronin, 2018: Earth's outgoing longwave radiation linear due to H_2O greenhouse effect. *Proc. Natl. Acad. Sci. USA*, **115**, 10 293–10 298, https://doi.org/10.1073/pnas.1809868115.

Kwok, R., 2018: Arctic sea ice thickness, volume, and multiyear ice coverage: Losses and coupled variability (1958–2018). *Environ. Res. Lett.*, **13**, 105005, https://doi.org/10.1088/1748-9326/aae3ec.

——, and N. Untersteiner, 2011: The thinning of Arctic sea ice. *Phys. Today*, **64**, 36–41, https://doi.org/10.1063/1.3580491.

Langen, P., R. Graversen, and T. Mauritsen, 2012: Separation of contributions from radiative feedbacks to polar amplification on an aquaplanet. *J. Climate*, **25**, 3010–3024, https://doi.org/10.1175/JCLI-D-11-00246.1.

Liu, W., and A. Fedorov, 2019: Global impacts of Arctic sea ice loss mediated by the Atlantic meridional overturning circulation. *Geophys. Res. Lett.*, **46**, 944–952, https://doi.org/10.1029/2018GL080602.

McCusker, K., P. Kushner, J. Fyfe, M. Sigmond, V. Kharin, and C. Bitz, 2017: Remarkable seperability of circulation response to Arctic sea ice loss and greenhouse gas forcing. *Geophys. Res. Lett.*, **44**, 7955–7964, https://doi.org/10.1002/2017GL074327.

Merlis, T., and M. Henry, 2018: Simple estimates of polar amplification in moist diffusive energy balance models. *J. Climate*, **31**, 5811–5824, https://doi.org/10.1175/JCLI-D-17-0578.1.

Mori, M., Y. Kosaka, M. Watanabe, H. Nakamura, and M. Kimoto, 2019: A reconciled estimate of the influence of Arctic sea ice loss on recent Eurasian cooling. *Nat. Climate Change*, **9**, 123–129, https://doi.org/10.1038/s41558-018-0379-3.

Notz, D., and Coauthors, 2020: Arctic sea ice in CMIP6. *Geophys. Res. Lett.*, **47**, e2019GL086749, https://doi.org/10.1029/2019GL086749.

Oudar, T., E. Sanchez-Gomez, F. Chauvin, J. Cattiaux, L. Terray, and C. Cassou, 2017: Respective roles of direct GHG radiative forcing and induced Arctic sea ice loss on the Northern Hemisphere atmospheric circulation. *Climate Dyn.*, **49**, 3693–3717, https://doi.org/10.1007/s00382-017-3541-0.

Overland, J., and Coauthors, 2021: How do intermittency and simultaneous processes obfuscate the Arctic influence on midlatitude winter extreme weather events. *Environ. Res. Lett.*, **16**, 043002, https://doi.org/10.1088/1748-9326/abdb5d.

Peings, Y., Z. Labe, and G. Magnusdottir, 2021: Are 100 ensemble members enough to capture the remote atmospheric response to +2°C Arctic sea ice loss? *J. Climate*, **34**, 3751–3769, https://doi.org/10.1175/JCLI-D-20-0613.1.

Petrie, R., L. Shaffrey, and R. Sutton, 2015: Atmospheric impact of Arctic sea ice loss in a coupled ocean–atmosphere simulation. *J. Climate*, **28**, 9606–9622, https://doi.org/10.1175/JCLI-D-15-0316.1.

Ramaswamy, V., and Coauthors, 2001: Radiative forcing of climate change. *Climate Change 2001: The Scientific Basis*, J. T. Houghton et al., Eds., Cambridge University Press, 349–416.

Ringgaard, I., S. Yang, E. Kaas, and J. Christensen, 2020: Barents–Kara sea ice and European winters in EC-Earth. *Climate Dyn.*, **54**, 3323–3338, https://doi.org/10.1007/s00382-020-05174-w.

Roach, L., I. Eisenman, T. Wagner, E. Blanchard-Wrigglesworth, and C. Bitz, 2022: Asymmetry in the seasonal cycle of Antarctic sea ice driven by insolation. *Nat. Geosci.*, **15**, 277–281, https://doi.org/10.1038/s41561-022-00913-6.

Ronalds, B., E. Barnes, and P. Hassanzadeh, 2018: A barotropic mechanism for the response of jet stream variability to Arctic amplification and sea ice loss. *J. Climate*, **31**, 7069–7085, https://doi.org/10.1175/JCLI-D-17-0778.1.

Rose, B., K. Armour, D. Battisti, N. Feldl, and D. Koll, 2014: The dependence of transient climate sensitivity and radiative feedbacks on the spatial pattern of ocean heat uptake. *Geophys. Res. Lett.*, **41**, 1071–1078, https://doi.org/10.1002/2013GL058955.

Russotto, R., and M. Biasutti, 2020: Polar amplification as an inherent response of a circulating atmosphere: Results from the TRACMIP aquaplanets. *Geophys. Res. Lett.*, **57**, e2019GL086771, https://doi.org/10.1029/2019GL086771.

Scinocca, J., M. Reader, D. Plummer, M. Sigmond, P. Kushner, T. Shepherd, and A. Ravishankara, 2009: Impact of sudden Arctic sea ice loss on stratospheric polar ozone recovery. *Geophys. Res. Lett.*, **36**, L24701, https://doi.org/10.1029/2009GL041239.

Screen, J., and R. Blackport, 2019: How robust is the atmospheric response to projected Arctic sea ice loss across climate models? *Geophys. Res. Lett.*, **46**, 11 406–11 415, https://doi.org/10.1029/2019GL084936.

——, and Coauthors, 2018: Consistency and discrepancy in the atmospheric response to Arctic sea-ice loss across climate models. *Nat. Geosci.*, **11**, 155–163, https://doi.org/10.1038/s41561-018-0059-y.

Semmler, T., L. Stulic, T. Jung, N. Tilinina, C. Campos, S. Gulev, and D. Koracin, 2016: Seasonal atmospheric responses to reduced Arctic sea ice in an ensemble of coupled model simulations. *J. Climate*, **29**, 5893–5913, https://doi.org/10.1175/JCLI-D-15-0586.1.

Senftleben, D., A. Lauer, and A. Karpechko, 2020: Constraining uncertainties in CMIP5 projections of September Arctic sea ice extent with observations. *J. Climate*, **33**, 1487–1503, https://doi.org/10.1175/JCLI-D-19-0075.1.

Sévellec, F., A. Fedorov, and W. Liu, 2017: Arctic sea-ice decline weakens the Atlantic meridional overturning circulation. *Nat. Climate Change*, **7**, 604–610, https://doi.org/10.1038/nclimate3353.

Shaw, T., and Z. Smith, 2022: The midlatitude response to polar sea ice loss: Idealized slab-ocean aquaplanet experiments with thermodynamic sea ice. *J. Climate*, **35**, 2633–2649, https://doi.org/10.1175/JCLI-D-21-0508.1.

Sherwood, S. C., and Coauthors, 2020: An assessment of Earth's climate sensitivity using multiple lines of evidence. *Rev. Geophys.*, **58**, e2019RG000678, https://doi.org/10.1029/2019RG000678.

Sime, L., P. Hopcroft, and R. Rhodes, 2019: Impact of abrupt sea ice loss on Greenland water isotopes during the last glacial period. *Proc. Natl. Acad. Sci. USA*, **116**, 4099–4104, https://doi.org/10.1073/pnas.1807261116.

Simon, A., G. Gastineau, C. Frankignoul, C. Rousset, and F. Codron, 2021: Transient climate response to Arctic sea ice loss with two ice-constraining methods. *J. Climate*, **34**, 3295–3310, https://doi.org/10.1175/JCLI-D-20-0288.1.

Smith, D., N. Dunstone, A. Scaife, E. Fiedler, D. Copsey, and S. Hardiman, 2017: Atmospheric response to Arctic and Antarctic sea ice: The importance of ocean–atmosphere coupling and the background state. *J. Climate*, **30**, 4547–4565, https://doi.org/10.1175/JCLI-D-16-0564.1.

——, and Coauthors, 2019: The Polar Amplification Model Intercomparison Project (PAMIP) contribution to CMIP6: Investigating the causes and consequences of polar amplification. *Geosci. Model Dev.*, **12**, 1139–1164, https://doi.org/10.5194/gmd-12-1139-2019.

Sun, L., M. Alexander, and C. Deser, 2018: Evolution of the global coupled climate response to Arctic sea ice loss during 1990–2090 and its contribution to climate change. *J. Climate*, **31**, 7823–7843, https://doi.org/10.1175/JCLI-D-18-0134.1.

——, C. Deser, and M. Alexander, 2020: Global coupled climate response to polar sea ice loss: Evaluating the effectiveness of different ice-constraining approaches. *Geophys. Res. Lett.*, **47**, e2019GL085788, https://doi.org/10.1029/2019GL085788.

Tomas, R., C. Deser, and L. Sun, 2016: The role of ocean heat transport in the global climate response to projected Arctic sea ice loss. *J. Climate*, **29**, 6841–6859, https://doi.org/10.1175/JCLI-D-15-0651.1.

Wagner, T., and I. Eisenman, 2015a: How climate model complexity influences sea ice stability. *J. Climate*, **28**, 3998–4014, https://doi.org/10.1175/JCLI-D-14-00654.1.

——, and ——, 2015b: False alarms: How early warning signals falsely predict abrupt sea ice loss. *Geophys. Res. Lett.*, **42**, 10 333–10 341, https://doi.org/10.1002/2015GL066297.

——, ——, and H. Mason, 2021: How sea ice drift influences sea ice area and volume. *Geophys. Res. Lett.*, **48**, e2021GL093069, https://doi.org/10.1029/2021GL093069.

Wang, K., C. Deser, L. Sun, and R. Tomas, 2018: Fast response of the tropics to an abrupt loss of Arctic sea ice via ocean dynamics. *Geophys. Res. Lett.*, **45**, 4264–4272, https://doi.org/10.1029/2018GL077325.

Zappa, G., F. Pithan, and T. Shepherd, 2018: Multimodel evidence for an atmospheric circulation response to Arctic sea ice loss in the CMIP5 future projections. *Geophys. Res. Lett.*, **45**, 1011–1019, https://doi.org/10.1002/2017GL076096.

Supporting Information for "Spurious climate warming in sea ice loss simulations from artificial Arctic heating"

M. R. England[1,2,3], I. Eisenman[3], T. J. W. Wagner[2,4]

[1]Department of Earth and Planetary Sciences, University of California Santa Cruz, Santa Cruz, California, USA

[2]Department of Physics and Physical Oceanography, University of North Carolina Wilmington, North Carolina, USA.

[3]Scripps Institution of Oceanography, University of California San Diego, La Jolla, California, USA.

[4]Department of Atmospheric and Oceanic Sciences, University of Winsconsin Madison, Madison, Wisconsin, USA.

Contents of this file

1. Text S1 to S2

2. Table S1

3. Figures S1 to S3

Text S1: Determining the Northern Hemisphere average and latitudinal structure of the annual-mean surface temperature response in the idealized model

We first take the Northern Hemisphere (NH) average, denoted by <>, of Equation 4 in the main text. Due to the equatorial boundary condition, the NH-mean atmospheric heat transport term is zero, such that:

$$A + B(< \overline{T_s} > -T_f) - F - F_b =< \overline{(1-\alpha)S} > . \tag{S1}$$

The deviation from the NH-mean (i.e., the latitudinal structure) is denoted by $'$, such that $\overline{T}_s' = \overline{T}_s - < \overline{T}_s >$. By subtracting Equation S1 from Equation 4, we get an equation in terms of the the deviation from the NH-mean:

$$B\overline{T_s}' - D\nabla^2\overline{T_s}' = \overline{(1-\alpha)S}', \tag{S2}$$

which is equivalent to Equation 5 in the main text. In Section 3, the only difference between the CONTROL and FUTURE simulations is an increase in the climate forcing F from 0 to 3.1 Wm^{-2}, which can be thought of as applying a perturbation ΔF to the CONTROL simulation. We recast Equation S1 in terms of this perturbation to get the following equation for the change in NH-mean annual-mean surface temperature $\Delta < \overline{T_s} >$:

$$\Delta < \overline{T_s} >= \frac{\Delta F - \Delta < \overline{\alpha S} >}{B}. \tag{S3}$$

Similarly, we recast Equation S2 in terms of the perturbation which gives the following implicit equation for the change in the deviation from the NH-mean annual-mean surface

temperature $\Delta\overline{T_s}'$, i.e., the change in its latitudinal structure:

$$B\Delta\overline{T_s}' - D\nabla^2(\Delta\overline{T_s}')) = -\Delta\overline{\alpha S}', \tag{S4}$$

which is equivalent to Equation 6 in the main text.

Note that deriving an analytic solution for $\Delta\overline{T_s}'$ is complicated by the dependence of albedo on surface temperature and by the Laplacian. It could be achieved by first solving Equation S4 for $\overline{\alpha S}'$ and then finding an expression for $\Delta\overline{T_s}'$ as a Legendre polynomial. For our purposes, however, Equation 5 and 6 are sufficient to illustrate our main points and gain a conceptual understanding of the behaviour of the idealized model.

Text S2: Preventing sea ice loss in a warmer climate. Although most previous studies have imposed sea ice conditions from a warmer climate into a control climate, a number of studies have alternatively investigated the same question by fixing sea ice conditions under a warming climate (Sun et al. 2018, Dai et al. 2019). In this case the effect of sea ice loss is estimated as the residual between the warming simulation in which sea ice is free to evolve and the warming simulation in which sea ice is fixed. To see if this directionality influences our results, we repeated our experiments using the three methodologies to impose sea ice conditions from the CONTROL simulation in the FUTURE simulation. These simulations are listed in Table S1, and the results are plotted in Fig. S3a. All of the methodologies artificially cool the high latitudes to fix the sea ice to CONTROL conditions (Fig. S3b). The annual-mean surface response to sea ice loss (Fig. S4), as determined by fixing sea ice cover in a warmer climate, is very similar to that diagnosed from imposing future sea ice conditions in a control climate (Fig. 3). Overall, the same conclusions can be drawn: namely that these widely used methods overestimate the impact of sea ice loss and other factors. Whether these methodologies are used to melt the ice to force sea ice loss, or to cool the surface to force sea ice growth, they similarly overestimate the climate response to sea ice changes.

References

Dai, A., Luo, D., Song, M., & Liu, J. (2019). Arctic amplification is caused by sea-ice loss under increasing CO2. Nature Communications, 10 (121). doi: 10.1038/s41467-018-07954-9

Sun, L., Alexander, M., & Deser, C. (2018). Evolution of the global coupled climate response to Arctic sea ice loss during 1990–2090 and its contribution to climate change. Journal of Climate, 31, 7,823-7,843. doi: 10.1175/JCLI-D-18-0134.1

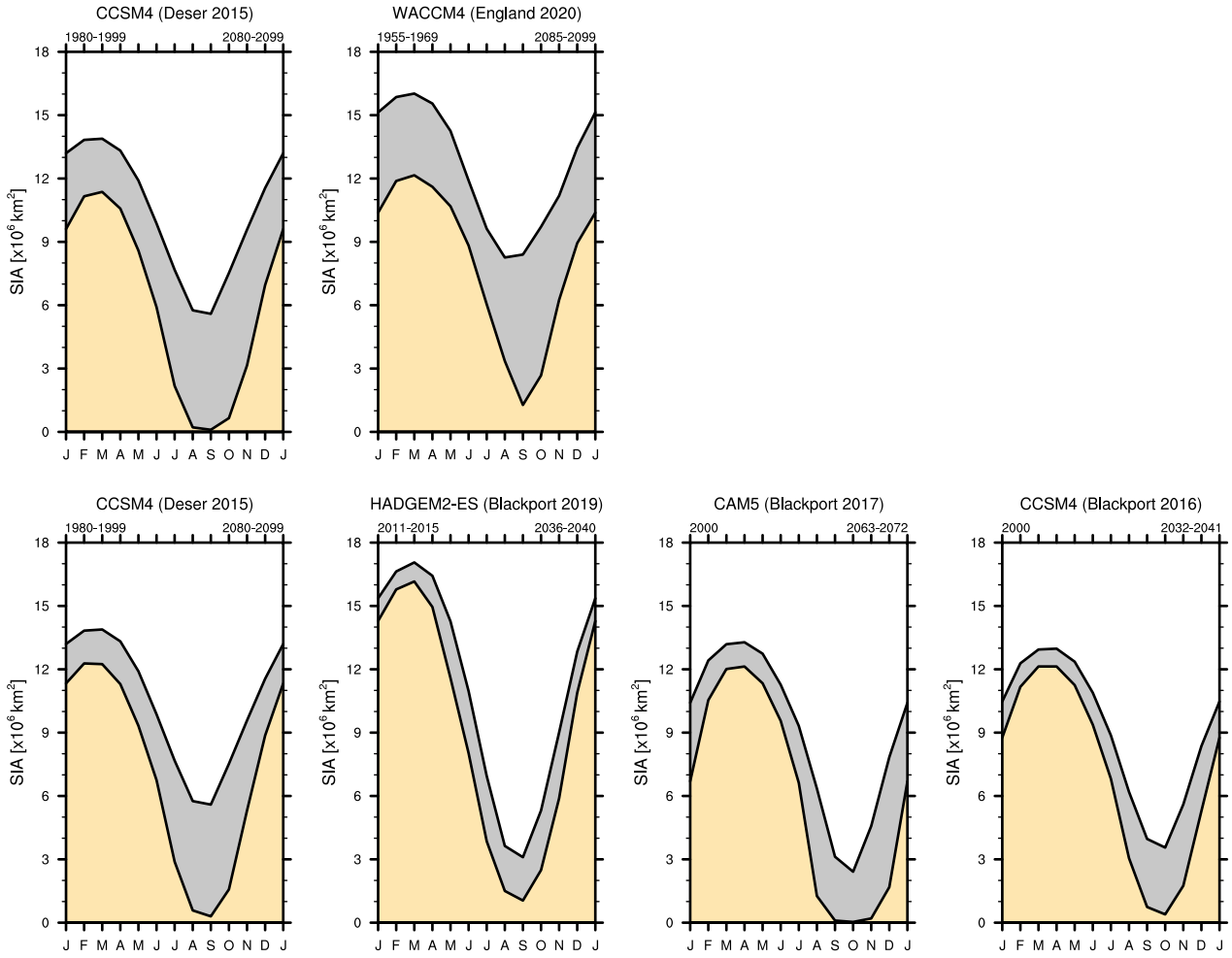

Figure S1. Seasonal cycle of sea ice area for control runs and future runs for a range of six sea ice loss simulations using comprehensive climate models. The top row shows the two simulations using the ghost flux methodology and the bottom row shows the four simulations using the albedo modification methodology. The grey shading shows the loss of sea ice area between the control and future simulations, and the yellow shading shows the sea ice area remaining in the future simulations. The reference period indicated in the top left is for the control simulation, and in the top right it is for the future simulation.

Table S1. Description of additional fixed sea ice simulations performed using the WE15 energy balance model.

Simulation	**Climate forcing [$\mathbf{Wm^{-2}}$]**	**Modification**
CONTROL_ICE_SPECIFIED_ALBEDO	3.1	Surface albedo specified from CONTROL
CONTROL_ICE_ALBEDO$_{summer}$	3.1	Albedo of sea ice increased from α_i=0.6 to α_i=0.65
CONTROL_ICE_ALBEDO$_{annual}$	3.1	Albedo of sea ice increased from α_i=0.6 to α_i=0.67
CONTROL_ICE_NUDGING	3.1	In gridboxes which are currently ice-free but are ice-covered in CONTROL, enthalpy is set to zero and then nudged to the target thickness with a timescale of 20 days.
CONTROL_ICE_GHOST_FLUX	3.1	60 Wm^{-2} of cooling applied to gridboxes which are ice-covered but are ice-free in FUTURE

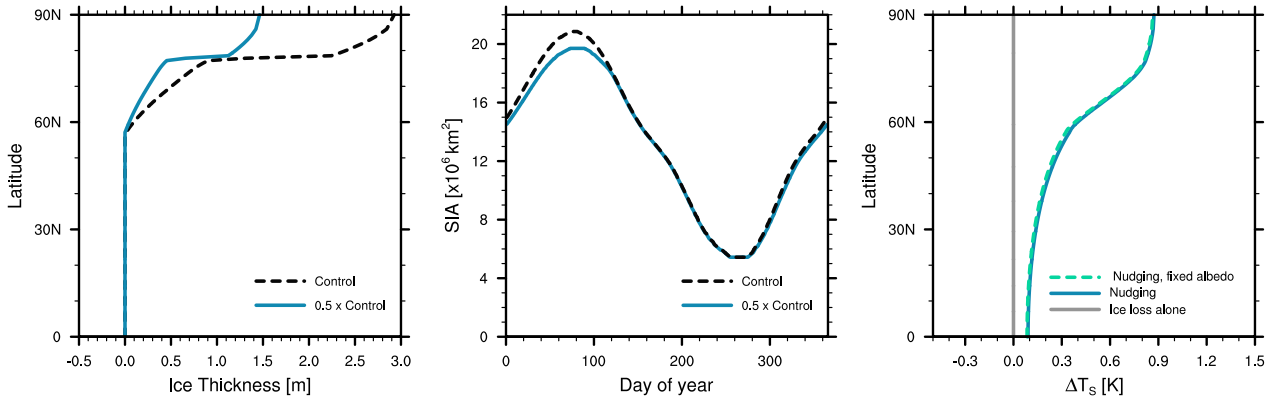

Figure S2. (a) Annual-mean latitudinal ice thickness profile for the a control simulation with $F = 0$ (black) and a nudging experiment in which, in grid cells with sea ice ($E < 0$) the enthalpy E is nudged to half of the enthalpy value from the CONTROL run (blue). In practice this means nudging the sea ice cover to be half as thick everywhere. (b) The seasonal cycle of the sea ice edge in CONTROL and 0.5 nudged thickness simulations. Crucially here, the sea ice area and hence ice edge does not change much. Remember, we know analytically that in this model the only influence sea ice has on the annual mean climate is through albedo changes – and the surface albedo is forced to be identical between the CONTROL and 0.5 thickness nudged simulation. Therefore, the role of ice loss alone should be close to zero because the albedo is relatively unchanged. This is illustrated in the grey line in panel c. However, the difference in surface temperature between the 0.5 thickness nudged simulation and the CONTROL is a robust surface warming (blue line panel c), which arises because we effectively added latent heat by removing the ice. The difference between the blue and gray line is due to this artificial heating, not sea ice loss. To be clear, the notion that reducing ice thickness does not impact the annual mean climate is only applicable in our idealized model and would not hold in a more complex model. We repeated the identical nudging experiment but with surface albedo specified from CONTROL, to check if any of the spurious response in panel c (blue line) is in fact driven by the small albedo changes in panel b, and this is shown in the dashed green line in panel c. As can be seen from comparing the dashed green line and blue line in panel c, the warming response is driven nearly entirely by the nudging, not the albedo change.

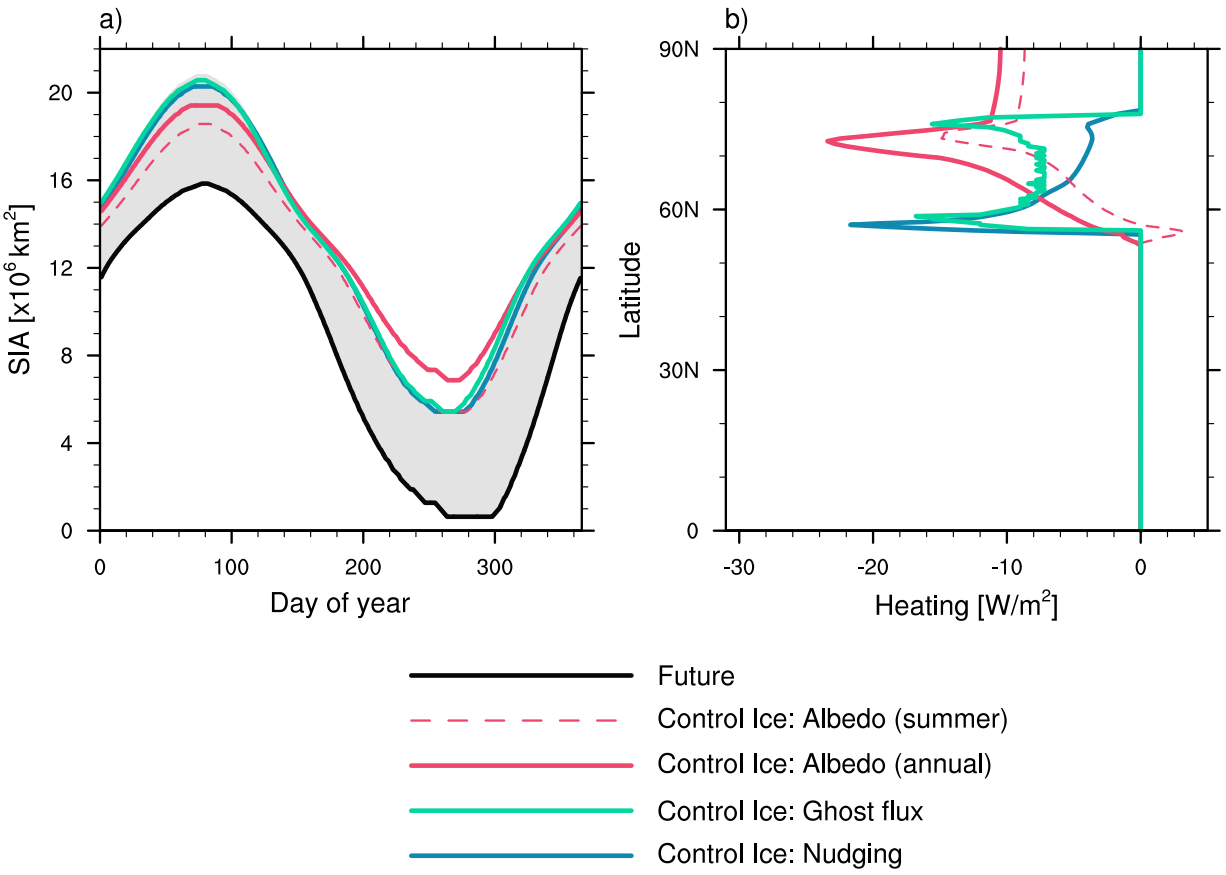

Figure S3. As in Fig. 2 but for the WE15 simulations with sea ice fixed to CONTROL conditions under FUTURE climate forcing, rather than being fixed to FUTURE sea ice conditions under CONTROL climate forcing.

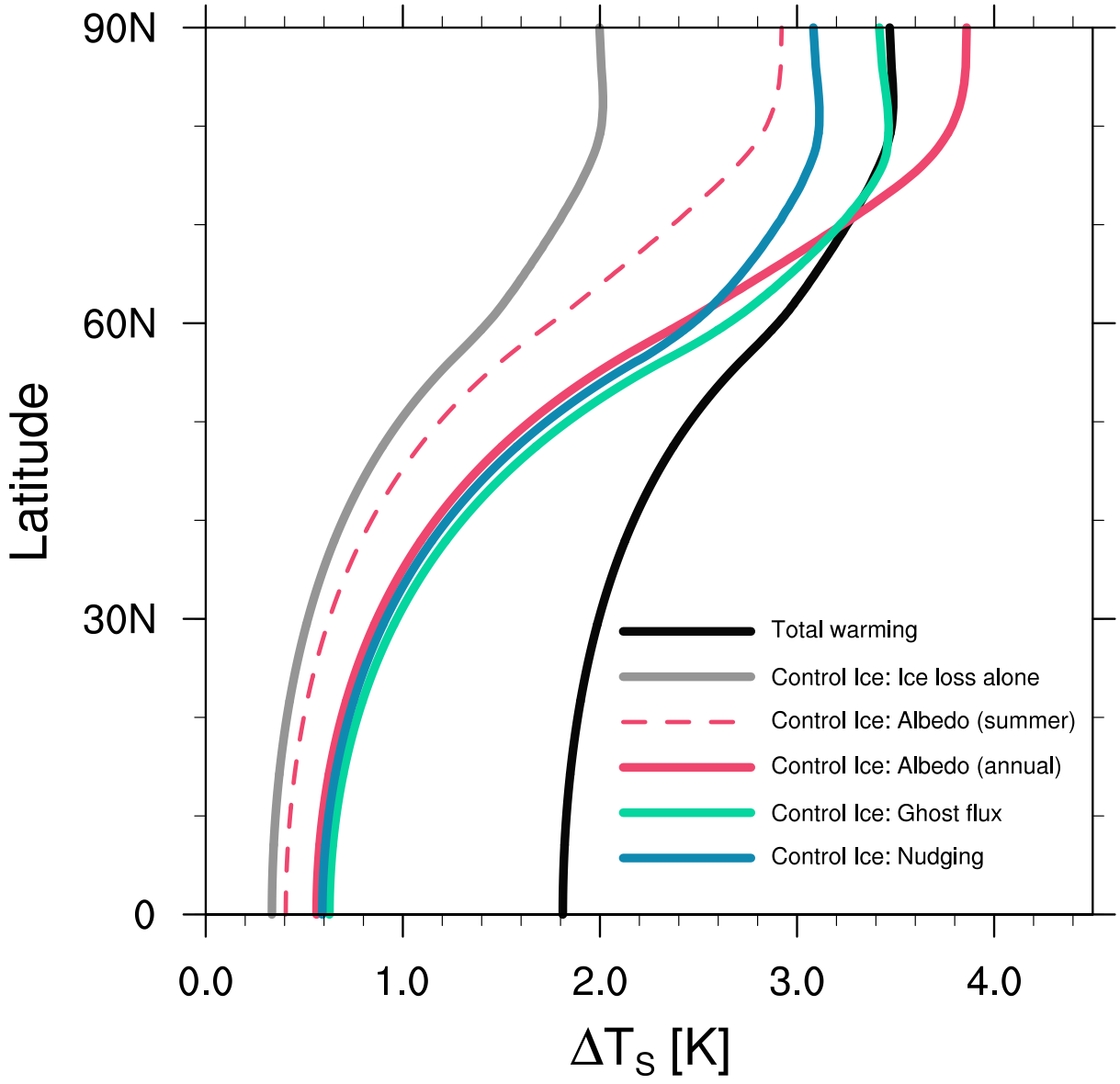

Figure S4. As in Fig. 3 but for the WE15 simulations shown in Fig. S3.